RSC Advances

PAPER

View Article Online
View Journal | View Issue

Check for updates

Cite this: *RSC Adv.*, 2026, **16**, 7830

Penicurvularins A and B, macrolides from an ascomycete fungus *Alternaria* sp.

Peinan Fu,[a] Xi Ren,[a] Qiaoling Wang,[a] Feng Guo,[a] Tingnan Zhou[b] and Zhiyang Lv*[a]

Received 25th December 2025
Accepted 19th January 2026

DOI: 10.1039/d5ra09998f

rsc.li/rsc-advances

Two new macrolides, penicurvularins A and B (**1** and **2**), and the three known compounds (**3**–**5**) were isolated from cultures of the ascomycete fungus *Alternaria* sp. Their structures were elucidated primarily by NMR experiments. The absolute configuration of **1** was assigned from electronic circular dichroism calculations. Compounds **1** and **5** are active against aquatic pathogenic bacteria *Vibrio alginolyticus* and *V. harveyi* with MIC values ranging from 4 to 8 μg mL^{-1}, while compound **5** is cytotoxic against tumor cell lines Huh7, 786-O, and 5673 with IC_{50} values of 11.6, 10.7, and 3.5 μM, respectively.

Introduction

Macrolides are a structurally diverse and biologically significant class of natural products characterized by a macrocyclic lactone ring, typically containing 12–16 carbon atoms or more.[1] These compounds have been extensively studied for their broad spectrum of biological activities, including antibacterial,[2,3] antifungal,[4,5] antiparasitic,[6] anti-inflammatory[7,8] and anti-tumor[9] properties. Since the discovery of erythromycin in the 1950s,[10] macrolides have played a pivotal role in pharmaceutical development, particularly in the treatment of infectious diseases.[11] Beyond their clinical applications, macrolides have also garnered attention as lead compounds for drug discovery and as probes for investigating cellular processes.[12]

Curvularin-type polyketides represent another intriguing class of fungal secondary metabolites, characterized by a 12-membered macrocyclic lactone fused to a resorcylic acid moiety.[13–15] These compounds, exemplified by curvularin and its analogues, have been reported to exhibit a range of bioactivities. The biosynthesis of curvularins involves iterative type I polyketide synthases (PKSs), and their structural diversity is often attributed to post-PKS modifications such as oxidation and methylation.[16] Despite their relatively simple structures compared with other macrolides, curvularins have shown promising potential as chemical scaffolds for bioactive molecule development.[15] During our continuous search for new bioactive metabolites from the ascomycete fungus fungi,[17–19] a strain of *Alternaria* sp. isolated from a soil sample collected from the Qinghai-Tibetan plateau, Tibet, People's Republic of China, was grown in a solid-substrate fermentation culture. An ethyl acetate (EtOAc) extract of the culture showed cytotoxic effects towards a small panel of three tumor cell lines. Fractionation of the extract afforded two new macrolides, which we named penicurvularins A and B (**1** and **2**; Fig. 1), and the three known compounds 5-methoxycurvularin,[20] curvularin[21] and dehydrocurvularin[22] (**3**–**5**; Fig. 1). Details of the isolation, structure elucidation, and bioactivity screening of these compounds are reported herein.

Results and discussion

Penicurvularin A (**1**) was assigned a molecular formula of $C_{22}H_{22}O_6$ (12 degrees of unsaturation) by HRESIMS. Its IR spectrum showed the presence of hydroxyl (3420 cm^{-1}), an ester carbonyl (1715 cm^{-1}) groups. Analysis of its NMR data (Table 1) revealed the presence of two methyl groups, four methylene, one oxymethines, 14 aromatic carbons with six oxygenated (δ_C 148.4, 150.7, 153.9, 155.3, 156.3 and 157.7) and five protonated, and one carboxylic carbon (δ_C 171.6). These data accounted for all of the NMR resonances and suggested that **1** was a tetracyclic compound. The ^{1}H–^{1}H COSY NMR data showed three isolated spin-system of C-10–C-11, C-13–C-16 and C-3′–C-4′ (Fig. 2). The HMBC correlations from H-6 to C-4, C-5, C-7, C-8 and C-9, and from H_2-2 to C-1, C-3, C-4 and C-8, a 1,2,3,5,6-

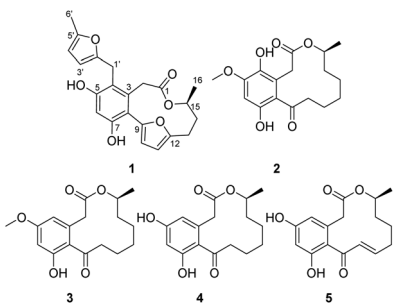

Fig. 1 Structures of compounds **1**–**5**.

[a]*School of Pharmacy, Jiangsu Food and Pharmaceutical Science College, Huaian 223003, People's Republic of China. E-mail: lvpharm@163.com*

[b]*Institute of Medicinal Biotechnology, Chinese Academy of Medical Sciences & Peking Union Medical College, Beijing 100730, People's Republic of China*

Open Access Article. Published on 06 February 2026. Downloaded on 2/13/2026 1:26:27 AM. This article is licensed under a Creative Commons Attribution-NonCommercial 3.0 Unported Licence.

© 2026 The Author(s). Published by the Royal Society of Chemistry

Open Access Article. Published on 06 February 2026. Downloaded on 2/13/2026 1:26:27 AM.
This article is licensed under a Creative Commons Attribution-NonCommercial 3.0 Unported Licence.

Table 1 NMR data of **1** and **2**

	1		**2**	
No.	δ_C[a], type	δ_H[b] (*J* in Hz)	δ_C[a], type	δ_H[b] (*J* in Hz)
1	171.6, qC		174.9, qC	
2	37.7, CH_2	3.71, d (14.8) 2.84, d (14.8)	32.8, CH_2	3.96 d (13.5) 3.64 d (13.5)
3	139.5, qC		120.9, qC	
4	117.7, qC		136.4, qC	
5	157.7, qC		152.7, qC	
6	102.1, CH	6.51, s	98.8, CH	6.52, s
7	155.3, qC		148.8, qC	
8	112.3, qC		122.5, qC	
9	148.4, qC		208.4, qC	
10	107.3, CH	6.11, d (3.0)	44.2, CH_2	3.12, m 2.57, m
11	111.0, CH	6.25, d (3.0)	24.6, CH_2	1.80, m 1.36, m
12	156.3, qC		27.9, CH_2	1.52, m 1.21, m
13	26.4, CH_2	2.85, m 2.64, m	25.3, CH_2	1.51, m 1.21, m
14	37.2, CH_2	2.02, m 1.76, m	31.9, CH_2	1.56, m
15	72.9, CH	5.10, m	75.6, CH	4.86, m
16	21.4, CH_3	1.20, d (6.4)	20.4, CH_3	1.24, d (5.8)
1′	25.6, CH_2	4.18, d (16.2) 3.88, d (16.2)		
2′	153.9, qC			
3′	106.9, CH	5.70, d (2.9)		
4′	106.9, CH	5.82, d (2.9)		
5′	150.7, qC			
6′	13.5, CH_3	2.18, s		
5-OCH_3			56.2, CH_3	3.75, s

[a] Recorded at 600 MHz. [b] Recorded at 150 MHz.

pentasubstituted phenyl unit fusing at C-3/C-8 was deduced. Correlations from H-10 and H-11 to C-9 and C-12, from H_2-13 to C-12, and from H-15 to C-1, plus the chemical shift values for C-9, C-12 and C-15 (δ_C 148.4, 156.3 and 72.9), established a furan unit fused to the 5-methyl-1,6-dioxacycloundecan-7-one at C-9/C-12. Further correlations from H_2-1′ to C-4, C-2′ and C-3′, and from H_3-6′ to C-4′ and C-5′, plus the chemical shift values for C-2′ and C-5′ (δ_C 153.9 and 150.7) lead to the connection of 5-methylfuran-2-yl-methyl moiety to C-1′ *via* C-4. On the basis of these data, the gross structure of **1** was established as shown.

The absolute configuration of **1** was deduced by comparison of the experimental and simulated electronic circular dichroism

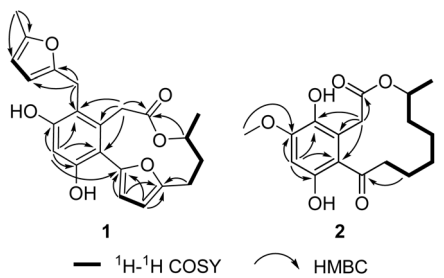

Fig. 2 Key ^{1}H–^{1}H COSY and HMBC correlations of **1** and **2**.

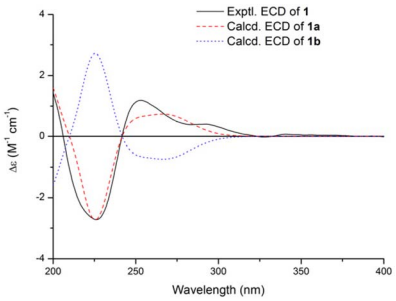

Fig. 3 Experimental ECD spectrum of **1** in MeOH and the calculated ECD spectra of **1a** and **1b**.

(ECD) spectra calculated using the time-dependent density functional theory (TDDFT)[23] for the (15*S*)-**1** (**1a**) and (15*R*)-**1** (**1b**) enantiomers. A systematic conformational analysis for **1a** was performed using the OPLS3 molecular mechanics force field followed by reoptimization at the B3LYP/6-311G(d, p) level afforded the lowest energy conformers (Fig. S11). The overall calculated ECD spectra of **1a** was then generated according to Boltzmann weighting of its lowest energy conformers by its relative energies (Fig. 3). And the overall calculated ECD spectra of **1b** was generated with Specdis1.70 software according to its enantiomer of **1a**. The experimental ECD curve of **1** was nearly identical to that calculated for **1a**, suggesting the 15*S* absolute configuration for **1**.

Penicurvularin B (**2**) was determined to have a molecular formula of $C_{17}H_{22}O_6$ (7 of unsaturation) based on HRESIMS and the NMR data (Table 1), which is 16 mass units higher than that of **3**. Analysis of the ^{1}H and ^{13}C NMR data for **2** revealed the presence of structural features similar to those found in **3**, except that H-4 (δ_H 6.35) were absent. Considering the chemical shift values of C-4 (δ_C 136.4), the remaining exchangeable proton was assigned as OH-4 by default, which was confirmed by the HMBC correlation from H-2 and H-6 to C-4. Therefore, the gross structure of **2** was established. The ECD spectrum of **2** was nearly identical to that of **3** (Fig. S21), and rotation value of 2 {[a]$^{25}_D$ −79.9 (c 0.10, MeOH)} was consistent with the reported one {[a]$^{20}_D$ −43.9 (c 0.02, MeOH)},[20] indicating that the absolute configuration of **2** was the same as that of **3**.

The other known compounds **3**–**5** isolated from the crude extract were identified as 5-methoxycurvularin (**3**),[20] curvularin (**4**),[21] dehydrocurvularin (**5**),[22] respectively, by comparison of their NMR and MS data with those reported.

Compounds **1**–**5** were tested for cytotoxicity against three human tumor cell lines, Huh7 (hepatocellular carcinoma cells), 786-O (kidney cancer cells), 5673 (bladder cancer cell), compound **5** showed potent cytotoxic effects,[24] with IC_{50} values of 11.6, 10.7 and 3.5 μM, respectively (Table 2). Compounds **1**–**5** were aslo evaluated for antibacterial activities against two aquatic bacteria[25] *Vibrio alginolyticus* ATCC 33787, *V. harveyi* ATCC 33842. Compounds **1** and **5** exhibited inhibitory activities against the aquatic pathogens *V. alginolyticus* and *V. harveyi* with MIC values of 4–8 μg mL^{-1} (Table 3). Previously, curvularin and its derivatives were found to exhibit anti-inflammatory activity and other activities.[19,26] Among the compounds tested

Open Access Article. Published on 06 February 2026. Downloaded on 2/13/2026 1:26:27 AM. This article is licensed under a Creative Commons Attribution-NonCommercial 3.0 Unported Licence.

Table 2 Cytotoxicity of compounds **1–5**

	IC_{50} [a] (μM)		
Compound	Huh7	786-O	5673
1	NA[b]	NA[b]	NA[b]
2	NA[b]	NA[b]	NA[b]
3	NA[b]	NA[b]	NA[b]
4	NA[b]	NA[b]	NA[b]
5	11.6 ± 1.8	10.7 ± 1.2	3.5 ± 0.3
cisplatin[c]	5.2 ± 0.7	5.3 ± 0.5	4.5 ± 0.5

[a] IC_{50} values were averaged from at least three independent experiments. [b] No activity was detected at 50 μM. [c] Positive control.

Table 3 Antibacterial activities of compounds **1–5** (MIC, μg mL^{-1})[a]

	Compounds					
Strains	**1**	**2**	**3**	**4**	**5**	Chloramphenicol[c]
V. alginolyticus	4	NA[b]	NA[b]	NA[b]	4	0.5
V. harveyi	8	NA[b]	NA[b]	NA[b]	8	1

[a] MIC values were averaged from at least three independent experiments. [b] No activity was detected at 64 μg mL^{-1}. [c] Positive control.

(compounds **1–5**, Table 2), only compound **5** exhibited cytotoxic activity. It is worth noting that compound **5** has the α,β-unsaturated ketone functional group, but compounds **1–4** do not have such moiety. Therefore, the α,β-unsaturated ketone in compound **5** might be responsible for cytotoxic activity. The cytotoxic mechanism of action of the α,β-unsaturated carbonyl compounds normally involves Michael type addition.[27]

Experimental

General experimental procedures

Optical rotations were measured on a Rudolph Research Analytical automatic polarimeter, and UV data were recorded on a Shimadzu Biospec-1601 spectrophotometer. CD spectra were recorded on a JASCO J-815 spectropolarimeter (solvent: MeOH; measure range: 400–200 nm; accumulations: 2; cell length: 1 mm; temperature: 25 °C; bandwidth: 1.00 nm; scanning speed: 100 nm min; concentration: 0.1). IR data were recorded using a Nicolet Magna-IR 750 spectrophotometer. ^1H and ^{13}C NMR spectra were acquired with Bruker Avance III-600 spectrometers using solvent signals (Acetone-d_6: δ_H 2.05/δ_C 29.84; $CDCl_3$: δ_H 7.26/δ_C 77.16) as references. The HSQC and HMBC experiments were optimized for 145.0 and 8.0 Hz, respectively. ESIMS and HRESIMS data were obtained on an Agilent Accurate-Mass-Q-TOF LC/MS G6550 instrument equipped with an ESI source. HPLC analysis and separation were performed using an Agilent 1260 instrument equipped with a variable-wavelength UV detector.

Fungal material

The culture of *Alternaria* sp. isolated from a soil sample collected from the Qinghai-Tibetan plateau, Tibet, People's Republic of China, in 2009. The isolate was identified based on morphology and sequence (GenBank Accession No. ON310806) analysis of the ITS region of the rDNA. The fungal strain was cultured on slants of potato dextrose agar (PDA) at 25 °C for 10 days. Agar plugs were cut into small pieces (about 0.5 × 0.5 × 0.5 cm^3) under aseptic conditions, and 25 pieces were used to inoculate in five 250 mL Erlenmeyer flasks, each containing 50 mL of media (0.4% glucose, 1% malt extract, and 0.4% yeast extract), and the final pH of the media was adjusted to 6.5 and sterilized by autoclave. Five flasks of the inoculated media were incubated at 25 °C on a rotary shaker at 170 rpm for 5 days to prepare the seed culture. Fermentation was carried out in 40 Fernbach flasks (500 mL) each containing 80 g of rice. Distilled H_2O (120 mL) was added to each flask, and the contents were soaked overnight before autoclaving at 15 psi for 30 min. After cooling to room temperature, each flask was inoculated with 5.0 mL of the spore inoculum and incubated at 25 °C for 40 days.

Extraction and isolation

The fermentation material was extracted repeatedly with EtOAc (4 × 4.0 L), and the organic solvent was evaporated to dryness under vacuum to afford 15.3 g of crude extract. The crude extract was fractionated by silica gel vacuum liquid chromatography (VLC) using petroleum ether–CH_2Cl_2–EtOAc–MeOH gradient elution. The fraction (1.5 g) eluted with 7:3 CH_2Cl_2–EtOAc was separated by reversed-phase silica gel column chromatography (CC) eluting with a MeOH–H_2O gradient. The fraction (258 mg) eluted with 45% MeOH–H_2O was further separated by Sephadex LH-20 CC eluting with MeOH, and the resulting subfractions were combined and purified by semi-preparative reversed-phase (RP) HPLC (Agilent Zorbax SB-C18 column; 5 mm; 9.4 × 250 mm; 48% MeOH in H_2O for 35 min; 3 mL min^{-1}) to afford **5** (20.5 mg, t_R 18.5 min) and **4** (100.2 mg, t_R 31.6 min). The fraction (1.3 g) eluted with 3:2.

CH_2Cl_2–EtOAc was separated by reversed-phase silica gel CC eluting with a MeOH–H_2O gradient. The fraction (100 mg) eluted with 60% MeOH–H_2O was further separated by Sephadex LH-20 CC eluting with MeOH, and the resulting subfractions were combined and purified by semipreparative RP HPLC (Agilent Zorbax SB-C18 column; 5 mm; 9.4 × 250 mm; 65% MeOH in H_2O for 35 min; 3 mL per min) to afford **2** (4.5 mg, t_R 10.0 min), **3** (2.1 mg, t_R 11.5 min), and **1** (3.5 mg, t_R 30.5 min).

Penicurvularin A (**1**). white amorphous powder; $[\alpha]^{25}_D$ +16.0 (*c* 0.1, MeOH); UV (MeOH) λ_{max} (log ε) 204 (3.50), 290 (3.68) nm; CD (*c* 3.3 × 10^{-4} M, MeOH) λ_{max} (Δε) 226 (−2.73), 253 (+1.19), 294 (+0.40) nm; IR (neat) ν_{max} 3420, 2933, 1715, 1608, 1250, 1164, 1053 cm^{-1}; ^1H and ^{13}C NMR data see Table 1; HMBC data (Acetone-d_6, 600 MHz) H_2-2 → C-1, 3, 4, 8; H-6 → C-4, 5, 7, 8, 9; H-10 → C- 9, 12; H-11 → C-9, 12; H-13 → C- 12; H-15 → C-1; H_3-16 → C-14, 15; H_2-1′ → C-3, 4, 5, 2′ 3′; H-3′ → C-2′, 4′, 5′; H-4′ → C-2′, 3′, 5′; H_3-6′ → C-4′, 5′; HRESIMS *m*/*z* 383.1483 $[M + H]^+$ (calcd for $C_{22}H_{23}O_6$, 383.1489).

Penicurvularin B (**2**). white amorphous powder; $[\alpha]^{25}_D$ −79.9 (*c* 0.1, MeOH); UV (MeOH) λ_{max} (log ε) 208 (3.91), 238 (3.75), 316 (3.43) nm; CD (*c* 2.0 × 10^{-4} M, MeOH) λ_{max} (Δε) 216 (−2.35), 243 (+3.61), 290 (−10.71) 358 (−1.99) nm; IR (neat) ν_{max} 3361, 2941, 1697, 1596, 1271, 1127, 1021 cm^{-1}; ^1H and ^{13}C NMR data see

© 2026 The Author(s). Published by the Royal Society of Chemistry

Open Access Article. Published on 06 February 2026. Downloaded on 2/13/2026 1:26:27 AM. This article is licensed under a Creative Commons Attribution-NonCommercial 3.0 Unported Licence.

Table 1; HMBC data ($CDCl_3$, 600 MHz) H_2-2 → C-1, 3, 4, 8; H-6 → C-4, 5, 7, 8, 9; H_2-11 → C-9; H_2-12 → C-10; H_2-13 → C-14; H_2-14 → C-12, 13, 16; H_3-16 → C-14, 15; OCH_3-5 → C-5; HRESIMS *m/z* 323.1485 $[M + H]^+$ (calcd for $C_{17}H_{23}O_6$, 323.1489).

Computational details

Conformational analyses for **1** within an energy window of 3.0 kcal mol^{-1} were performed by using the OPLS3 molecular mechanics force field. A total of 19 conformers were obtained. The conformers were then further optimized with the software package Gaussian 09 at the B3LYP/6-311G(d, p) level. The dominant conformers were evaluated according to the optimization energy and the populations were provided in Table S1. And then the 60 lowest electronic transitions for the obtained dominant conformers were calculated using time-dependent density functional theory (TD-DFT) methods at the CAM-B3LYP/6-311G(d, p) level. ECD spectra of the conformers were simulated using a Gaussian function. The overall theoretical ECD spectra were obtained according to the Boltzmann weighting of each dominant conformer.[28]

Cytotoxicity assays. MTT assays were performed as previously described.[24] Briefly, cells were seeded into 96-well plates at a density of 5 × 103 cells per well for 24 h and were exposed to different concentrations of test compounds. After incubation for 72 h, cells were stained with 25 μL of MTT solution (5 mg per mL) for 25 min. Finally, the mixture of medium and MTT solution was removed, and 75 μL of DMSO was added to dissolve formazan crystals. Absorbance of each well was measured at 544 nm (test wavelength) and 690 nm (background) using the multi-mode microplate reader. Background was subtracted from the absorbance of each well. Cisplatin was used as the positive control three duplicate wells were used for each concentration, and all the tests were repeated three times.

Antimicrobial assay. The antibacterial activities against two aquatic bacteria *Vibrio alginolyticus* ATCC 33787, and *V. harveyi* ATCC 33842, were carried out by a serial dilution technique using 96-well microtiter plates.[25] The final concentrations of the test compound in the well were 64, 32, 16, 8, 4, 2, 1, and 0.5 μg per mL. Chloramphenicol was used as the positive control.

Conclusions

In summary, two new macrolides, penicurvularins A and B (**1** and **2**), and the three known compounds 5-methoxycurvularin, curvularin, and dehydrocurvularin (**3**–**5**) were isolated from cultures of the ascomycete fungus *Alternaria* sp. Their structures were elucidated based on NMR spectroscopic data and electronic circular dichroism (ECD) calculations. Compound **1** represents the first example of curvularin derivative featuring a unique 5-methylfuran-2-yl-methyl and a furan moiety. Compound **2** is structurally related to 5-methoxycurvularin (**3**), but differs by having a hydroxyl group at C-4. Compounds **1** and **5** are active against aquatic pathogenic bacteria *Vibrio alginolyticus* and *V. harveyi* with MIC values ranging from 4 to 8 μg mL^{-1}, while compound **5** is cytotoxic against tumor cell lines Huh7, 786-O, and 763 with IC_{50} values of 11.6, 10.7, and 3.5 μM, respectively.

Conflicts of interest

The authors declare no conflict interest.

Data availability

The authors confirm that the data supporting the findings of this study are available within the article [and/or] its supplementary information (SI). Supplementary information: UV, IR, HRESIMS, NMR spectra of compounds **1**; ECD calculations of compounds **1**. See DOI: https://doi.org/10.1039/d5ra09998f.

Acknowledgements

We gratefully acknowledge financial support from the Jiangsu Food & Pharmaceutical Science College (302320230555) and Jiangsu Province Shuangchuang Doctor Program (JSSCBS0573).

Notes and references

1 A. Evidente, *Nat. Prod. Rep.*, 2022, **39**, 1591–1621.
2 C. X. Wang, R. Ding, S. T. Jiang, J. S. Tang, D. Hu, G. D. Chen, F. Lin, K. Hong, X. S. Yao and H. Gao, *J. Nat. Prod.*, 2016, **79**, 2446–2454.
3 P. R. Koliye, A. N Bissoue, E. N. M. Mouelle, S. K. Nguikwie, C. V. Z. Owona, V. E. Simons, S. H. Akone, L. M. Meva'a, R. Kalscheuer and Z. Naturforsch, *C J. Biosci.*, 2024, **79**, 371–376.
4 I. Pérez-Victoria, D. Oves-Costales, R. Lacret, J. Martín, M. Sánchez-Hidalgo, C. Díaz, B. Cautain, F. Vicente, O. Genilloud and F. Reyes, *Org. Biomol. Chem.*, 2019, **17**, 2954–2971.
5 Z. Yu, L. Wang, J. Yang, F. Zhang, Y. Sun, M. Yu, Y. Yan, Y. Ma and S. Huang, *Tetrahedron Lett.*, 2016, **57**, 1375–1378.
6 K. Umeda, A. Iwasaki, R. Taguchi, N. Kurisawa, G. Jeelani, T. Nozaki and K. Suenaga, *J. Nat. Prod.*, 2023, **86**, 2529–2538.
7 F. H. Al-Awadhi, S. Kokkaliari, R. Ratnayake, V. J. Paul and H. Luesch, *J. Nat. Prod.*, 2024, **87**, 2355–2365.
8 Y. Wu, Z. Zhang, Y. Zhong, J. Huang, X. Li, J. Jiang, Y. Deng, L. Zhang and F. He, *RSC Adv.*, 2017, **7**, 40015–40019.
9 J. S. An, H. J. Lim, J. Y. Lee, Y. J. Jang, S. J. Nam, S. K. Lee and D. C. Oh, *J. Nat. Prod.*, 2022, **85**, 936–942.
10 F. R. Heilman, W. E. Herrell, W. E. Wellman and J. E. Geraci, *Proc. Staff Meet Mayo Clin.*, 1952, **27**, 285–304.
11 K. D. Lenz, K. E. Klosterman, H. Mukundan and J. Z. Kubicek-Sutherland, *Toxins*, 2021, **13**, 347.
12 C. A. Miller, J. M. Ho, S. E. Parks and M. R. Bennett, *ACS Synth. Biol.*, 2021, **10**, 258–264.
13 K. Arai, B. J. Rawlings, Y. Yoshizawa and J. C. Vederas, *J. Am. Chem. Soc.*, 1989, **111**, 3391–3399.
14 J. Zhan, E. M. K. Wijeratne, C. J. Seliga, J. Zhang, E. E. Pierson, L. S. Pierson III, H. D. Vanetten and A. A. L. Gunatilaka, *J. Antibiot.*, 2004, **57**, 341–344.

Open Access Article. Published on 06 February 2026. Downloaded on 2/13/2026 1:26:27 AM.
This article is licensed under a Creative Commons Attribution-NonCommercial 3.0 Unported Licence.

15 A. H. Aly, A. Debbab, C. Clements, R. Edrada-Ebel, B. Orlikova, M. Diederich, V. Wray, W. Lin and P. Proksch, *Bioorgan. Med. Chem.*, 2011, **19**, 414–421.
16 B. J. Rawlings, *Nat. Prod. Rep.*, 2001, **18**, 190–227.
17 E. Li, F. Zhang, S. Niu, X. Liu, G. Liu and Y. Che, *Org. Lett.*, 2012, **14**, 3320–3323.
18 J. Zhang, L. Liu, B. Wang, Y. Zhang, L. Wang, X. Liu and Y. Che, *J. Nat. Prod.*, 2015, **78**, 3058–3066.
19 X. Hou, Y. Xu, S. Zhu, Y. Zhang, L. Guo, F. Qiu and Y. Che, *RSC Adv.*, 2020, **10**, 15622–15628.
20 Z. Deng, A. Deng, D. Luo, D. Gong, K. Zou, Y. Peng and Z. Guo, *Nat. Prod. Commun.*, 2015, **10**, 1277–1278.
21 E. L. Ghisalberti, D. C. R. Hockless, C. Y. Rowland and A. H. White, *Aust. J. Chem.*, 1993, **46**, 571–575.
22 E. L. Ghisalerti and C. Y. Rowland, *J. Nat. Prod.*, 1993, **56**, 2175–2177.
23 S. Zhu, F. Ren, Z. Guo, J. Liu, X. Liu, G. Liu and Y. Che, *J. Nat. Prod.*, 2019, **82**, 462–468.
24 N. Zhang, Y. Chen, R. Jiang, E. Li, X. Chen, Z. Xi, Y. Guo, X. Liu, Y. Zhou, Y. Che and X. Jiang, *Autophagy*, 2011, **7**, 598–612.
25 C. G. Pierce, P. Uppuluri, A. R. Tristan, F. L. Wormley Jr, E. Mowat, G. Ramage and J. L. Lopez-Ribot, *Nat. Protoc.*, 2008, **3**, 1494–1500.
26 R. R. Banala, S. K. Vemuri, S. Ev, G. R. Av and S. Gpv, *Asian Spine J.*, 2021, **15**, 143–154.
27 Z. Fan, X. Zhao, M. Li, H. Wang and R. Huang, *Chem. Biodivers.*, 2025, **22**, e01583.
28 M. J. Frisch, G. W. Trucks, H. B. Schlegel, G. E. Scuseria, M. A. Robb, J. R. Cheeseman, G. Scalmani, V. Barone, B. Mennucci, G. A. Petersson, H. Nakatsuji, M. Caricato, X. Li, H. P. Hratchian, A. F. Izmaylov, J. Bloino, G. Zheng, J. L. Sonnenberg, M. Hada, M. Ehara, K. Toyota, R. Fukuda, J. Hasegawa, M. Ishida, T. Nakajima, Y. Honda, O. Kitao, H. Nakai, T. Vreven, J. A. Montgomery Jr, J. E. Peralta, F. Ogliaro, M. Bearpark, J. J. Heyd, E. Brothers, K. N. Kudin, V. N. Staroverov, R. Kobayashi, J. Normand, K. Raghavachari, A. Rendell, J. C. Burant, S. S. Iyengar, J. Tomasi, M. Cossi, N. Rega, J. M. Millam, M. Klene, J. E. Knox, J. B. Cross, V. Bakken, C. Adamo, J. Jaramillo, R. Gomperts, R. E. Stratmann, O. Yazyev, A. J. Austin, R. Cammi, C. Pomelli, J. W. Ochterski, R. L. Martin, K. Morokuma, V. G. Zakrzewski, G. A. Voth, P. Salvador, J. J. Dannenberg, S. Dapprich, A. D. Daniels, O. Farkas, J. B. Foresman, J. V. Ortiz, J. Cioslowski and D. J. Fox, *Gaussian 09, Rev D.01*, Gaussian, Inc.: Wallingford, CT, 2009.

© 2026 The Author(s). Published by the Royal Society of Chemistry